

DOTAREM (DOTA)–Gold-Nanoparticles: Design, Spectroscopic Evaluation to Build Hybrid Contrast Agents to Applications in Nanomedicine

Memona Khan¹, Hui Liu², Pasquale Sacco^{3,4}, Eleonora Marsich^{3,4}, Xiaowu Li², Nadia Djaker¹, Jolanda Spadavecchia¹

¹CNRS, UMR 7244, NBD-CSPBAT, Laboratory of Chemistry, Structures and Properties of Biomaterials and Therapeutic Agents University Paris 13, Sorbonne Paris Nord, Bobigny, France; ²Department of Hepatobiliary Surgery, Guangdong Provincial Key Laboratory of Regional Immunity and Diseases & Carson International Cancer Center, Shenzhen University General Hospital & Shenzhen University Clinical Medical Academy Center, Shenzhen University, Shenzhen, People's Republic of China; ³Department of Life Sciences, University of Trieste, Trieste, I-34127, Italy; ⁴Department of Medicine, Surgery and Health Sciences, University of Trieste, Trieste, I-34129, Italy

Correspondence: Nadia Djaker; Jolanda Spadavecchia, CNRS, UMR 7244, NBD-CSPBAT, Laboratory of Chemistry, Structures and Properties of Biomaterials and Therapeutic Agents University Paris 13, Sorbonne Paris Nord, Bobigny, France, Email nadia.djaker@univ-paris13.fr; jolanda.spadavecchia@univ-paris13.fr

Introduction: The realization of MRI contrast agents through chemical protocols of functionalization is a strong domain of research. In this work, we developed and formulated a novel hybrid gold nanoparticle system in which a gold salt (HAuCl_4) is combined with dotarem, an MRI contrast agent (DOTA) by chelation (Method IN) and stabilized by a lactose-modified chitosan polymer (CTL; Chitlac) to form DOTA IN-CTL AuNPs.

Result and Discussion: The authors demonstrate the biological efficiency of these nanoparticles in the case of three cell lines: Mia PaCa-2 (human pancreatic cancer cell line), TIB-75 (murine liver cell line) and KKU-M213 (cholangiocarcinoma cell line). DOTA IN-CTL AuNPs are stable under physiological conditions, are nontoxic, and are very efficient as PTT agents. The highlights, such as high stability and preliminary MRI in vitro and in vivo models, may be suitable for diagnosis and therapy.

Conclusion: We proved that DOTA IN-CTL AuNPs have several advantages: i) Biological efficacy on three cell lines: MIA PaCa-2 (human pancreatic cancer cell line), TIB-75 (murine liver cell line) and KKU-M213 (cholangiocarcinoma cell line); ii) high stability, and no-toxicity; iii) high efficiency as a PPT agent. The study conducted on MRI in vitro and in vivo models will be suitable for diagnosis and therapy.

Keywords: nanotheranostic, MRI, hybrid nanoparticles, dotarem, biomedical applications

Introduction

Hybrid gold nanoparticles have occupied a key role in the biochemical domain, thanks to their characteristics, which make them good perspectives for medical applications.^{1–4} Recently, the principal aim of the researchers has been targeted hybrid nanoparticles for multimodal imaging applications, also combined to therapy and imaging (theranostics).^{5–8} Lately, Spadavecchia et al, have realized several types of hybrid nanovectors based on a complexation methodology (Method IN).^{9–11} This chemical protocol was implemented to encapsulate some drugs, polymers and/or biomolecules^{12–14} with gold salts, through complexation and electrostatic interactions between peculiar chemical groups. Recently the same authors have conceived bimetallic nanovectors, formed by a complex between gadolinium ions (Gd^{3+}) and gold salt, encapsulated with a biocompatible polymer to generate a contrast agent nanoparticle^{10,15} with high quality magnetic resonance imaging (MRI) images in the diagnostic field.

The realization of MRI contrast agents through chemical protocols of functionalization is a strong domain of research.^{16–19} The application of nanoparticles loaded with high concentrations of gadolinium (Gd) therefore holds the potential to overcome the current sensitivity disadvantage of MRI as a diagnosis tool. Previous studies have proved and tested several nanoparticles with varying parameters such as shape, size and type of chemical functionalization, in order to study the advantages and disadvantages about “in vivo” pharmacokinetic parameters.²⁰ MRI contrast agents are employed in order to exploit the

precision and resolution of specific tissues analyzed in an MR image. Nevertheless Gd^{3+} is a toxic element responsible for the inhibition of several biological processes²¹ and inducing harmful effects. For this inconvenience several analyses were carried out in order to decrease this toxicity through the chemical functionalization of dotarem (DOTA).²² DOTA is a macrocyclic T1 contrast agent used in the MRI field.²³ This contrast agent is known as a non-toxic and effective improvement to the contrast of MRI images.¹⁶ The particularity of DOTA is to have gadolinium in the core and DOTA, around it as a protection (Figure S1 in Supporting Information). DOTA gives a great thermodynamic association constant compared to acyclic ligands.^{24–26} These characteristics are very important to safely use a gadolinium-based contrast agent in the field of biomedical imaging.²⁷ In the present study, we have realized a novel nano-diagnostic contrast agent for the first time: DOTA was complexed with a gold salt to form biocompatible hybrid gold nanoparticles (DOTA IN-CTL AuNPs). Thanks to this complexation methodology, DOTA will assume a better chemical and steric configuration in order to allow a good therapeutic efficacy. We also investigated their biological efficacy after internalisation in pancreatic MIA PaCa-2, KKU-M213 (cholangiocarcinoma cell) and hepatocytes TIB-75 cells in order to confirm a preliminary effect as an imaging contrast agent *in vivo*. The chemical-physical mechanism of degradation of this hybrid nanostructure was carried out to confirm a remarkable multitasking nanovector for further nano-medical applications such as multimodal cancer therapy and diagnostics. In this work, we also proved the possibility of using these particles as photothermal agents in the case of photothermal therapy (PTT). As gold-based nanoparticles, these plasmonic agents offer a high temperature elevation in their close-surface area. The temperature elevation between 4 °C and 11 °C (PTT window) after a few minutes allowed cancer cells destruction with 70% efficiency. In theranostic therapy these nanoparticles offer an opportunity to a new generation of nanoparticles dedicated to MRI imaging and cancer treatment by PTT.

Materials and Methods

The chemical compounds, tetrachloroauric acid ($HAuCl_4 \cdot 3H_2O$), gadolinium chloride hexahydrate ($GdCl_3 \cdot 6H_2O$), sodium borohydride ($NaBH_4$), were purchased from Sigma-Aldrich (Saint-Quentin Fallavier, France). The solution of DOTAREMR[®] (0.5 mmol/mL) was purchased from laboratories Guerbet, Aulnay sous Bois, France.

Hydrochloride CTL (Chitlac) was kindly provided by BiopoLife S.r.l. (Trieste, Italy).^{21,28,29}

Synthesis of DOTAREM-CTL-AuNPs Solution (DOTA IN-CTL AuNPs)

Preparation CTL Solution

CTL was solubilized at a concentration of 1 mg/mL in Milli-Q water (pH 6) under room temperature.

The synthesis of DOTA IN-CTL AuNPs was prepared by mixing 20 mL of aqueous $HAuCl_4$ solution (0.8 mM) with 5 mL of DOTA (1.3 mM) for 3 mins. Then, 5 mL of CTL solution (1 mg/mL) was added to the stirring solution. Finally, 1.8 mL of ice-cold 7.93 mM $NaBH_4$ was added dropwise. The resulting pink/violet solution was purified by ultracentrifugation and dialysis.⁹

Physical-Chemical Characterization

All measurements of characterization were carried out at least in triplicate in order to validate the reproducibility of the synthetic and analytical procedures.^{9,10}

UV-Vis Absorption Spectroscopy

The UV-vis absorption spectra of all samples were carried out by a double-beam Varian Cary 500 UV-vis spectrophotometer (Agilent, Les Ulis, France) under experimental conditions discussed previously.^{9,10}

Dynamic Light Scattering (DLS) and Zeta Potential Measurements

Hydrodynamic particles size distribution and zeta potential measurements were recorded on a Zetasizer Nano ZS (Malvern Instruments, Malvern, UK) equipped with a He-Ne laser (633 nm, fixed scattering angle of 173°) at room temperature.

Transmission Electron Microscopy (TEM)

Transmission electron microscopy (TEM) images of colloids were acquired with a JOEL JEM 1011 microscope operating (JOEL, Tokyo, Japan) at an acceleration voltage of 100 kV.

SERS

The Raman spectra were recorded on an Xplora spectrometer (Horiba Scientifics), which is equipped with a laser diode at 660 nm wavelength and 8 mW excitation power. The diffraction grating used is 600 features/mm which offers a spectral resolution of 12 cm^{-1} .

Preliminary MRI In Vivo Test (POC In Vivo)

Experimental procedures were conducted in accordance with the NIH and were approved by the Experimental Animal Ethics Committee of Guangzhou University of Chinese Medicine. In vivo tests were performed using male nude mice (strain: BALB/cA-Grade: SPF; age 5 weeks; mice production license number SCXK (Yue) 2018–0002, Guangdong Medical Laboratory Animal Center; mice certificate number no. 44007200064015; no. 44007200070200; mice use license number SYXK (Yue) 2018–0001, laboratory animal center, Guangzhou University of Chinese Medicine).

For this study we have used just 3 mice to see the efficiency of the contrast agent, DOTAREM complexed with gold nanoparticles. Some further studies with details are in progress. HUH7 human liver cancer cells inoculated in the flank (the total number of injected cells was 1.2×10^5), and administration was started 7 days after modeling, and the administration was continued for 3 weeks. After the formation of the tumor model of nude mice (tumor volume reached $150\text{--}200\text{ mm}^3$, about 7 days), 100 μL of each mouse was injected with a solution; DOTAREM (DOTA), CTL and DOTA IN-CTL AuNPs. The survival time of the tumor-bearing mice and all parameters were checked and recorded.

The T_1 and T_2 relaxation times of 3 solutions; DOTAREM (concentration of DOTA = 1.7 mM), CTL and DOTA IN-CTL AuNPs (concentration of DOTA = 1.3 mM), were performed on three mice at different times, pre-injection, 30 min, 1h and 2h.

In this work, in vivo experiments were carried out by recording T_1 and T_2 maps with a 3T magnetic resonance imaging (uPMR 790 PET/MR with the united compressed sensing (uCS) platform) equipped with a 45/200 high performance gradient; repetition time (RT) is 1052 ms and echo time (ET) is 12.28 ms. Slice thickness (ST) is 1.30 mm.

Sample Irradiation

The solutions (control and nanoparticles) were irradiated with an 808 nm continuous laser (FocusLight, China) at 0.75 W/cm^2 power density. The temperature elevation ΔT ($\Delta T = T(t) - T(0s)$) was measured over 15 min using a thermocouple probe (Hanna Instruments, USA) with an accuracy of $0.1\text{ }^\circ\text{C}$. The PTT set up was already described by the authors.^{30–32} The solutions volume (1 mL) and the irradiation surface (1 cm^2) were maintained at a constant during all the measurements.

For PTT experiments on cells, 24 wells of 4000 cells with 100 μL were incubated for 24 h in a 96-well culture plate at $37\text{ }^\circ\text{C}$ and 5% CO_2 . After 24h, in 12 wells, the DMEM medium was replaced by DOTA-AuNPs (2 nM) and 12 wells with H_2O as a control. After 24 h, 6 wells with DOTA IN-CTL AuNPs and 6 wells with H_2O were irradiated by an NIR laser. During the irradiation the cells were maintained at $37\text{ }^\circ\text{C}$. After the irradiation the solution DOTA-AuNPs and H_2O was removed and replaced by DMEM and incubated for another 24 h. Then cell growth inhibition was determined by measuring 3-(4,5-dimethylthiazol-2-yl)-2,5-diphenyltetrazolium bromide (MTT) dye absorbance by living cells. MTT solution (5 mg/mL in water) was added to each well and cells were incubated for 3 h. Formazan crystals resulting from MTT reduction were dissolved by the addition of 10% SDS in DMSO/acetic acid solution per well. The relative quantity of formazan products formed in each well was detected by reading absorbance at 570 nm. Cell growth was normalized to a control group without any treatment.

Cell Culture

Three cells lines were used: the tumor MIA PaCa-2 derived from surgical explant of a pancreas carcinoma from a 65-year-old Caucasian man, KKU-M213, a cholangiocarcinoma cell line established from the biliary tract of a 58-year-old man and

TIB-75 hepatocytes. Cell lines were purchased from American Type culture collection (ATCC) and cultured in DMEM (Gibco, Bio-Sciences Ltd, Ireland) supplemented with 10% FBS (Sigma-Aldrich) in a humidified atmosphere at 37 °C and 5% CO₂ and 95% air in a humidified atmosphere.

Cytotoxicity Tests

For the cytotoxicity tests, cells were plated into 96-wells at 4000 cells per well in 100 µL of culture medium. They were maintained in a 5% CO₂-humidity. 24 h after, the medium was removed and replaced by a new medium containing nanoparticles. Nine different concentrations of DOTA and DOTA IN-CTL AuNPs: 600 µM, 300 µM, 150 µM, 75 µM, 37 µM, 18.75 µM, 9.375 µM, 4.688 µM, 2.344 µM and 0 µM. The cytotoxicity was evaluated with MTT tests. The analyses were computed using GraphPad Prism software.

Stability of Hybrid Gold Nanoparticle Contrast Agent (DOTA IN-CTL AuNPs)

The stability of DOTA IN-CTL AuNPs was detected by UV-vis profiles and other techniques (DLS, PZ) 0.1 mL of colloidal solution at 2.4×10^{-4} M was dissolved in PBS and DMEM during 72–120 h. The experiments were repeated after 1 year with the same colloidal stock solution, without optochemical modification.

Release

DOTA releases were evaluated at physiological temperature (37 °C). DOTA-loaded CTL-AuNPs were dispersed at a concentration of 1.3×10^{12} particles/mL in 1.0 mL PBS and submitted for dialysis as previously described.⁹ After this experiment we did not observe the release of DOTA free at pH 7 from nanoparticles. Release and decomplexation tests were done under two pH conditions, pH 7 and pH 4. In order to do that, 500 µL of the nanoparticles solution was added into 1 mL of PBS at pH 7 and pH 4. The final solution was incubated at 37 °C and characterized by UV-vis at different times; 5 min, 1 h, 3 h, 6 h, 24 h and 96 h. In order to see visually the release of these nanoparticles, these solutions were characterized by TEM at different times; 1 h, 6 h and 24 h.

Results and Discussion

Formation Mechanism of DOTA IN-CTL AuNPs and Spectroscopic Validation

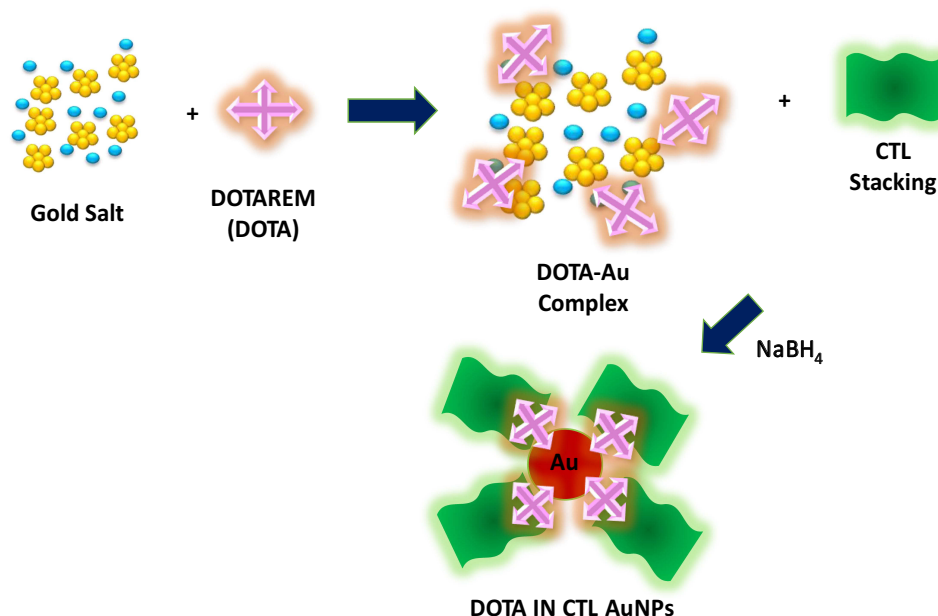
Previously many authors have developed bimetallic nanostructures based on Gd chelates and gold nanorods,⁸ Gd-oligonucleotides-AuNPs,¹⁹ and Gd chelates on hydroxyapatite³³ as multimodal MRI/CT contrast agents. Previously Spadavecchia et al, have studied the mechanism of bimetallic Au-Gd hybrid nano formulations and theranostic bimetallic-nanostructures for nanomedicine applications with highlights in photodynamic therapy.^{10,11} Based of this experimental proof, we applied our methodology (Method IN) to realize, for the first time, a hybrid gold nanoparticles, previous gold complexation of DOTA. In our case, the formation of hybrid gold NPs from DOTA and AuCl₄[−] follows the subsequent steps depicted in [Scheme 1](#):

- (1) Interaction of DOTA with AuCl₄[−] and initial formation of the DOTA-gold complex through carboxylate groups to produce hybrid DOTA gold cluster.
- (2) Electrostatic adsorption of CTL polymer (CTL) onto DOTA-AuCl₂ clusters.
- (3) Reduction of gold complex to form hybrid gold nanoparticles (DOTA IN-CTL AuNPs) and colloidal stabilization through the CTL and DOTA-Au molecules.

In the first step, DOTA was mixed in an aqueous gold salt solution (HAuCl₄) to form a complex with it. The addition of the CTL polymer in the DOTA -gold complex solution (DOTA-AuCl₂[−]) improves the complexation with the gold ions (second step).⁹ In the third step, the final reduction by NaBH₄ improves the growth process of DOTA nanoformulation.

The colloidal solution was characterized by UV-vis absorption spectroscopy, TEM and Raman spectroscopy.

We also estimated the steric arrangement of DOTA into gold nanoparticles (DOTA-AuNPs) without CTL polymer. Unfortunately the performed DOTA-AuNPs was unstable and precipitated after 24 h (see [Scheme S1](#) of reaction and UV-vis profile and [Figure S2 in Supporting Information](#)).



Scheme 1 Schematic design of the synthesis of DOTA IN-CTL AuNPs.

Concerning the spectroscopic evaluation of DOTA IN-CTL AuNPs: [Figure 1A](#), blue line displays the localized surface plasmon resonance (LSPR) bands of DOTA IN-CTL AuNPs with a strong resonance band at around 540 nm confirming the presence of spherical nanoparticles with a good dispersity ([Figure 1B](#)). The presence of the peak at 230 nm, confirms the presence of polymer embedded on the complex DOTA-AuCl₂. This optical characteristic, was related to π - π^* electronic transitions between the DOTA ring and AuCl₄⁻, indicating explicit evidence of the complex formation. TEM images showed a characteristic spherical shape ([Figure 1B](#)) with a diameter of about 18 nm (Zeta potential and DLS measurements show that DOTA IN-CTL AuNPs colloids were stable at physiological pH). This stability was enhanced with the presence of the CTL coating⁶ displaying a better stability in DMEM (5% BSA) during 24 h (see [Figure S3 in Supporting Information](#)).

DOTA IN-CTL AuNPs were also characterized by Raman spectroscopy ([Figure 1C](#)) in which we monitored all characteristic peaks of DOTA (403 cm⁻¹, and several bands between 600 and 1000 cm⁻¹) as control ([Figure 1C](#) black line).

In the case of DOTA IN-CTL AuNPs ([Figure 1C](#) blue line), Raman spectra showed a very intense peak at 610 cm⁻¹ and an improvement of the peaks in the range 342 cm⁻¹ and 480 cm⁻¹. These bands are due to the gold chloride stretches, δ (O-Au-O) and δ (-C-O-C) in the DOTA ring and Gd-Au confirming the presence of DOTA-AuCl₂ in solution. The spectral bands from 1200 cm⁻¹ to 1550 cm⁻¹ are responsible for the vibrations of N-H bending and C-N stretching, while the peaks between 1550 cm⁻¹ and 1750 cm⁻¹ correspond to the C=O stretching mode. The band at 836 cm⁻¹ is due to vibrations of the aromatic ring. All spectra also display several peaks at 324, 660 and 1630 cm⁻¹ due to vibrations of Gd-OH and Gd-Cl in a hybrid nanoparticle, as previously described.¹¹

Stability of DOTA IN-CTL AuNPs

The stability of DOTA IN-CTL AuNPs in solution, was carried out by monitoring the size and charge of nanoparticles by DLS/PZ at pH 7, pH 4 and in biological media (DMEM, BSA 5%). The synthesized DOTA IN-CTL AuNPs displays a minor optical change in the longitudinal band position over a period of 72 h at pH 7 ([Figure 2A](#)). Although the band intensity slightly decreased overtime, we assume that insignificant agglomeration occurred over 72 h, implying that DOTA IN-CTL AuNPs might find application as clinical nano-delivery systems. Zeta potential analysis confirmed the spectroscopic results, showing that DOTA IN-CTL AuNPs were stable at physiological pH (zeta-potential = +30 ± 1 mV

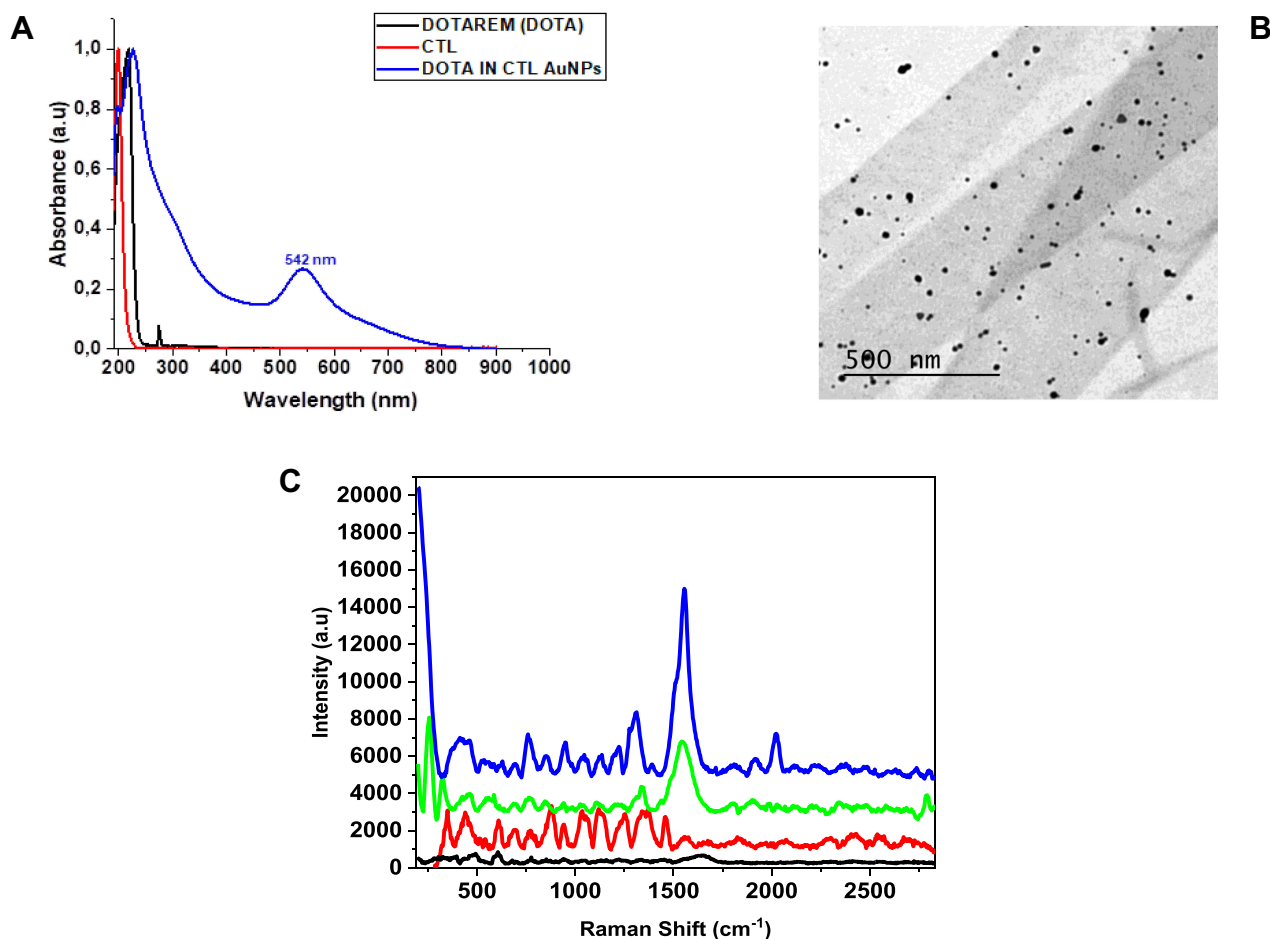


Figure 1 (A) Normalized UV-vis absorption spectrum of DOTA IN-CTL AuNPs (blue line) compared to free CTL (red line) and DOTA (black line) as controls. (B) TEM images of DOTA IN-CTL AuNPs; scale bars: 500 nm. (C) Raman spectrum of DOTA IN-CTL AuNPs (blue line) compared to free CTL (red line), DOTA (black line) and DOTA-AuNPs (without CTL) spectrum (green line) as controls. Experimental conditions: $\lambda_{exc} = 785$ nm; laser power 20 mW; accumulation time 180 s.

with a PDI equal to 0.331). The same experiment was repeated in the presence of DMEM (BSA 5%) during 120 h in dynamic UV-vis absorption spectra (Figure S2 in Supporting Information) displayed a red shift of plasmon peak (from 540 nm to 560 nm) after 5 min of incubation in DMEM due to electrostatic absorption of biological proteins into solution and successive stabilization of colloidal solution from 72 h to 120 h. In order to check the stability process, we also synthesized DOTA AuNPs without CTL polymer by method IN (Scheme S1 in Supporting Information) and monitored their optical properties by UV-vis (Figure S3 in Supporting Information). We observed a formation of small nanoparticles with a plasmon peak at 528 nm during 24 h. After this time, the colloidal solution precipitates with the disappearance of the plasmon peak (Figure S3 in Supporting Information). We assume that DOTA IN-CTL AuNPs enhanced stability is due to the presence of the CTL polymer chains on the nanoparticle surface.

Release of DOTA IN-CTL AuNPs

The size and shape of AuNPs is very important in nanomedicine because these parameters influence all pharmacokinetic parameters in the blood circulation.³⁴

In order to know the behavior of DOTA IN-CTL AuNPs as contrast agent candidates, in the nanomedicine field, comparative spectroscopic studies (UV-vis; Raman) were performed under specific conditions (pH 7 and 4; T: 37 °C) in order to check the DOTA release as gold complex under a range of times from 1 h to 96 h (Figures 2, S3 in Supporting Information).

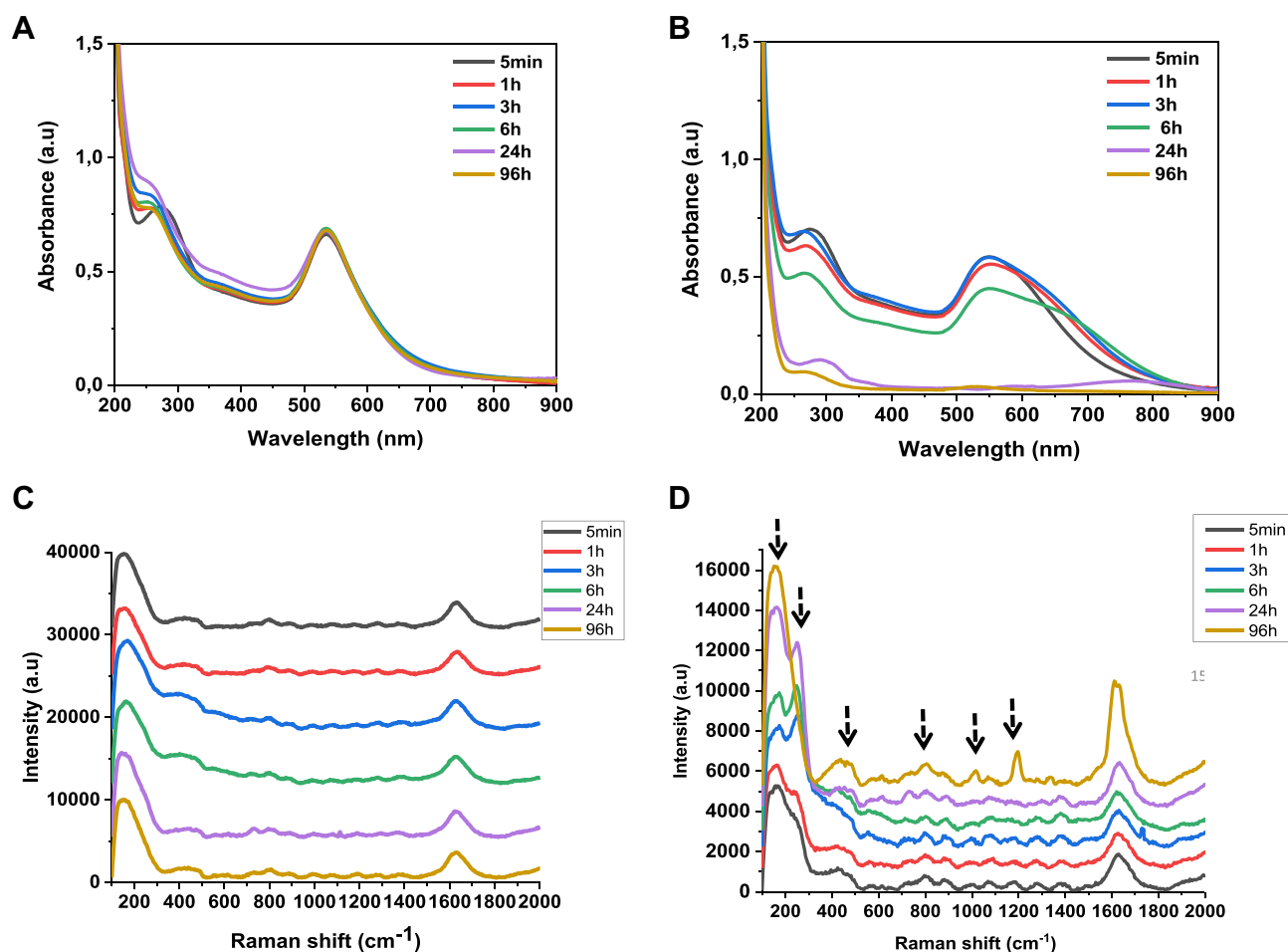


Figure 2 Stability profile and degradation/release changes in the UV-vis absorption (A and B) and Raman (C and D) spectra of DOTA IN-CTL AuNPs after incubation in buffer solution at pH 7 (A–C) and pH 4 (B–D) up to 96h.

We conceived and synthesized large hybrid gold nanoparticles and encapsulated them into biodegradable CTL polymer to form DOTA IN-CTL AuNPs. Thus, DOTA IN-CTL AuNPs was characterized by UV-vis and Raman spectroscopy after incubation for 96 h in PBS at pH 7 and pH 4 at 37 °C in order to (1) confirm the DOTA release as a gold-complex and (2) to evaluate variations in the chemical orientation of DOTA at pH 4 (when DOTA is protonated) and pH 7 (when DOTA is partially deprotonated). The resulting nanoparticles maintain their size and structure in the short term after incorporation in PBS at pH 7. Contrarily, at pH 4, the polymer degrades into intermediate products and we observe a decrease of size until they release the small gold cores for excretion^{14,15} (Figure 3 and Scheme 2). Figure 2A and B shows localized spectra plasmon (LSP) resonance before and after incubation of DOTA IN-CTL AuNPs under specific conditions (pH 4–7; time 96 h). At pH 7 (Figure 2A), the LSP remains unchanged at 540 nm confirming any release or degradation of our nanovector during 96 h. A different response is perceived at pH 4 (Figure 2B), in which we detect an amplification of the absorbance peak after 5 min of incubation. The optical phenomenon continues during 6 h with an evidence shoulder peak responsible for the colloidal aggregation. After 24 h, under some conditions, we observe a disappearance of the peak at 540 nm with a decrease of the peak at 256 nm. We assume that during incubation at pH 4, DOTA migrates in the polymer (CTL) chains and is released as DOTA-CTL-AuCl₂⁻ (Scheme 2) as described previously.¹⁴ This optical behaviour was confirmed by Raman spectroscopy (Figure 2C and D). Indeed at pH 7, the Raman spectra remains unchanged during the time (5 min–96 h) (Figure 2C), while at pH 4 we observe a progressive modification of the spectroscopic fingerprint of DOTA IN-CTL AuNPs in the time.

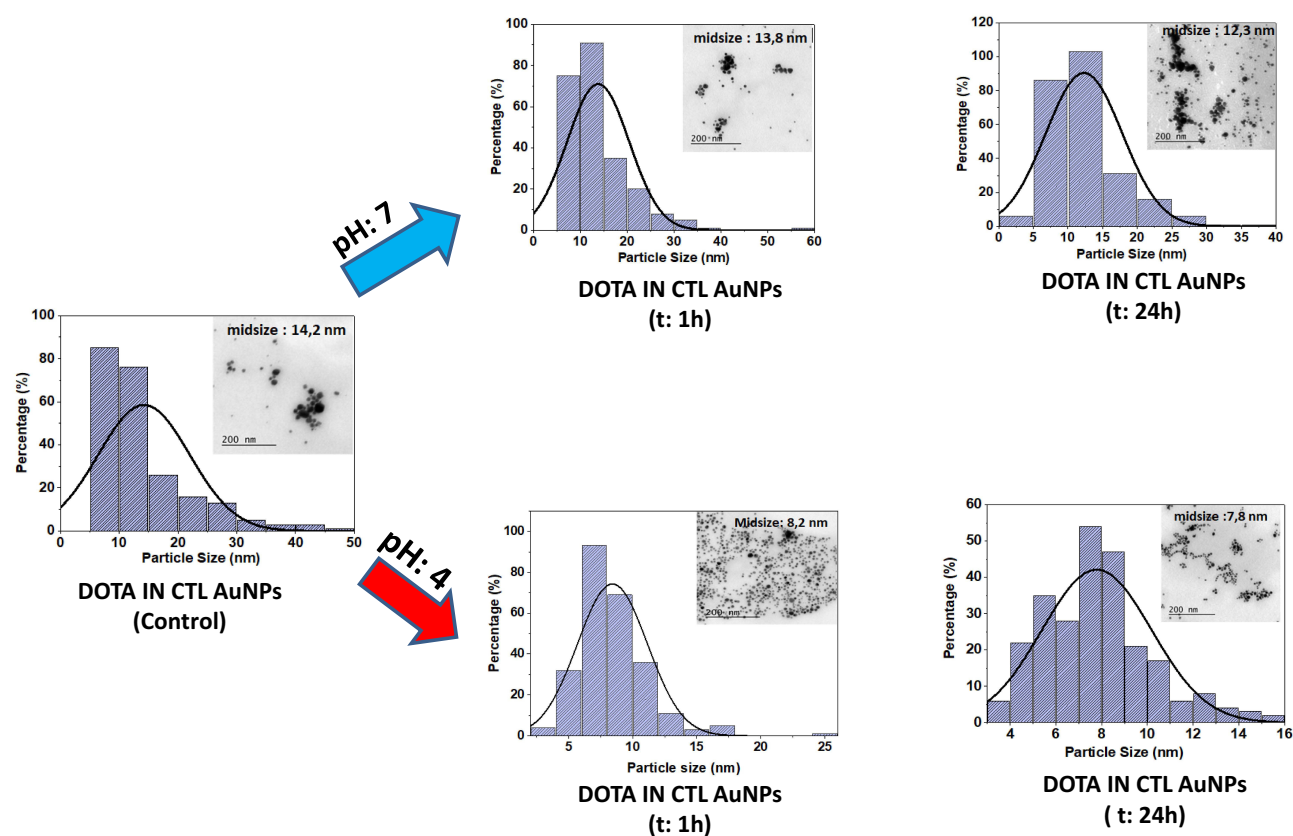
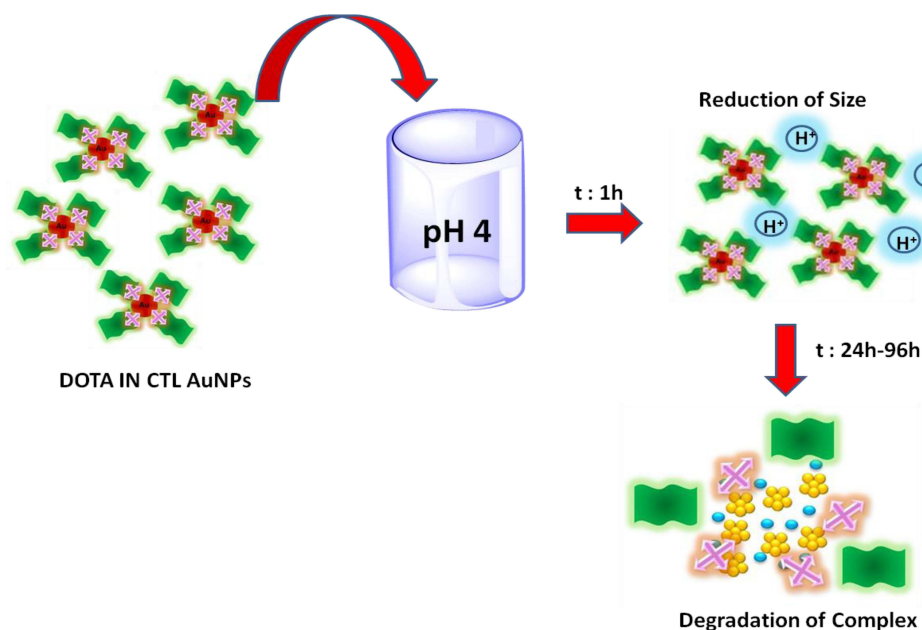


Figure 3 Size distribution histogram, TEM Images and conformational shape modifications of DOTA IN CTL AuNPs under PBS (37 °C) at pH 4 and pH 7.



Scheme 2 Depicted scheme of experimental test of colloidal degradation at pH 4 during 24h-96h.

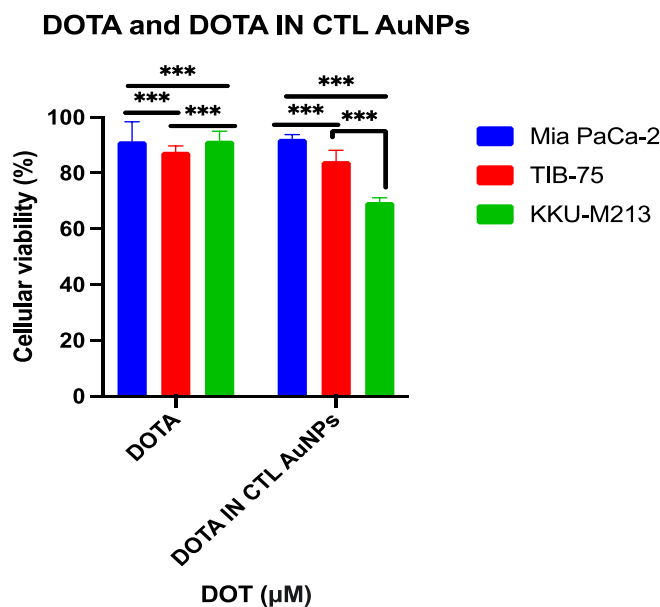
The Raman bands at 263 cm^{-1} and $240\text{--}282\text{ cm}^{-1}$ were monitored to evaluate the DOTA release, respectively, from AuNPs. The intensity of this band continuously modified overtime, with disappearance of the peak at 282 nm after 96 h (Figure 2D). Also, a strong Raman intensity increase after 24 h was observed in the spectral range $400\text{--}1800\text{ cm}^{-1}$, with

appearance of the novel peaks ($1019\text{--}1074\text{ cm}^{-1}$ and 1196 cm^{-1} , after 96 h due to C-O-C stretching in the backbone of CTL³⁵ confirming that, DOTA release and colloidal degradation were pH and time-dependent. About the release of DOTA, we have considered that 100% of DOTA is encapsulated into nanoparticles, and when during a degradation of the nanoparticles, DOTA is released under gold complex. At pH 4, only 15% of DOTA is released after 1 h, after 6 h the release is about 35% and after 24 h, 95% of DOTA is completely released with a consequent degradation of the nanoparticle. On the other hand at pH 7 we did not observe any release of DOTA as showed by UV-vis and Raman spectra.

We also observed a size variation of our nanovectors under pH 4 and 7 (Figure 3). If we compare both pH, we observe a negligible variation of size at pH 7 and a gradual reduction of size from 14 nm (as synthesized) to 7.8 nm after 24 h (pH 4) (Figure 3). This behaviour is very important to explain a favorable release and decomplexation of metallic nanoparticles with consequent fast elimination after injection. We conclude that, under pH conditions, a dramatic size change of DOTA IN-CTL AuNPs happened and DOTA was released as a gold complex, as previously described for other drugs.⁹

Cytotoxicity

The cytotoxicity of DOTA IN-CTL AuNPs was evaluated on three types of cell lines, TIB-75 (hepatocytes), KKU-M213 (cholangiocarcinoma cells) and MIA PaCa-2 (pancreatic cells), using the MTT cytotoxicity assay with increasing the concentration of DOTA in the nanoparticles from 0 to 600 μM (Figure 4). The choice of the cell lines is due to the comparison of two types of aggressive gastric cancers: adenocarcinoma pancreatic cancer (PDAC) and cholangiocarcinoma (CC). Both types of cancer represent a similitude about the anatomic position, the poor diagnostic and the metabolic and enzymatic ways implicated in carcinogenic phenomenon. The third line (TIB-75) was used as a control, derived from a simple hepatocarcinoma. All three MIA PaCa-2, TIB-75 and KKU-M213 cells were exposed to a range of DOTA IN-CTL AuNPs dilutions in complete media (DMEM+10% FBS) (concentrations ranging from 0 to 600 μM DOTA in DOTA IN-CTL AuNPs). To evaluate the potential toxicity of DOTA as a control substance, concentrations from 0 to 5.3 mM DOTA were investigated. The percentage of living cells (KKU-M213, MIA PaCa-2 and TIB-75) was evaluated by UV-vis spectroscopy after 24 h exposure to DOTA IN-CTL AuNPs and DOTA alone. Figure 4 shows the



Source of Variation	% of total variation	P value	P value summary	Significant?
Interaction	34.46	0.0004	***	Yes
Row Factor	23.03	0.0006	***	Yes
Column Factor	29.45	0.0008	***	Yes

Figure 4 Cell viability measurement for Anova analysis by MTT assay of Mia PaCa-2, TIB-75 and KKU-M213 after incubation with DOTA alone and hybrid nanoparticles (DOTA IN CTL-AuNPs). P values of less than 0.001 are flagged with asterisks that represent the significant difference between each histogram.

cytotoxicity of DOTA alone with an IC₅₀ greater than 5.2 mM for MIA PaCa-2, 5.4 mM for TIB-75 and 5.1 mM for KKKU-M213.

Note that, as one can see in the graph, the IC₅₀ is not reached, indicating that DOTA is not toxic to these cell lines.

Figure 4 shows the cytotoxicity of DOTA IN-CTL AuNPs with an IC₅₀ greater than 386 μ M for MIA PaCa-2, 305 μ M for TIB-75 and 258 μ M. Just like DOTA alone, we do not reach the IC₅₀, which means that our nanoparticles are not toxic to the cell lines. In summary, the cytotoxicity results of DOTA IN-CTL AuNPs were converted by calculating the IC₅₀ of the individual compounds such as CTL, DOTA and Au³⁺ of AuNPs. The results show that the DOTA complexed with gold nanoparticles is not toxic to the cells.

Photothermal Heating

In theranostic, the combination of MRI imaging and PTT therapy using iron, gadolinium or titanium based nanoparticles was already demonstrated in several works.^{36–39} In addition to its imaging properties as an MRI contrast agent, DOTA IN-CTL AuNPs shows high thermoplasmonic properties due to their gold nature during their irradiation under an 808 nm laser wavelength (Figure 5A). Despite the shift between the excitation wavelength (808 nm) and the nanoparticles LSPR (540 nm), PTT is very effective as already demonstrated in various published works.^{31,32,40,41} The temperature elevation ΔT ($\Delta T = T(t) - T(0s)$) in a solution of 2 nM DOTA IN-CTL AuNPs was recorded during 15 min, each 30 seconds. Figure 5B shows that ΔT increases rapidly after 2 min reaching the PTT start window at 4 °C, it continues to rise until 10 minutes to reach a plateau at 11 °C (the end of the PTT window)⁴² Note that the buffer solutions temperature elevation increased only by 1 °C. The PTT efficiency was measured by irradiating three cancerous cell lines: MIA PaCa-2, TIB-75

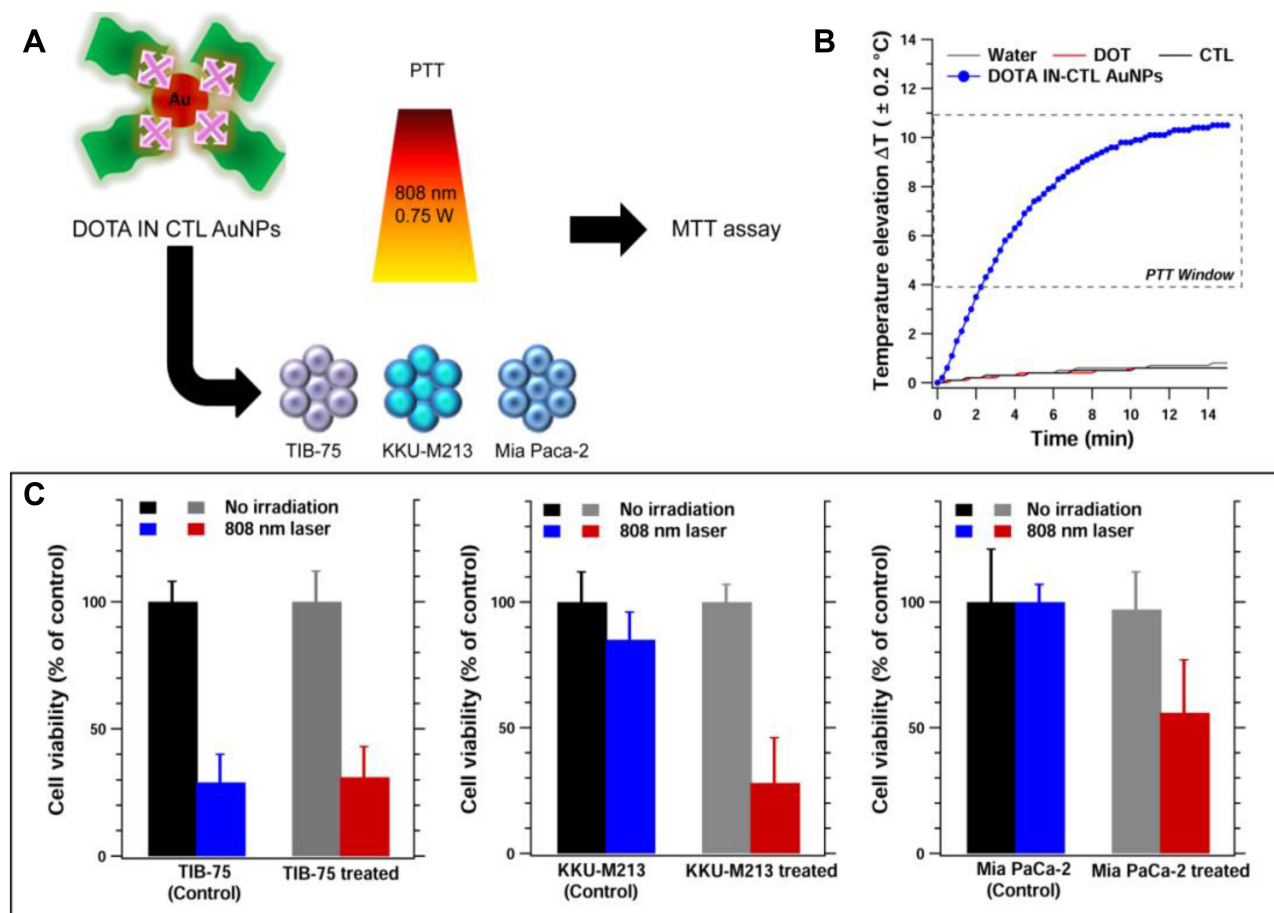
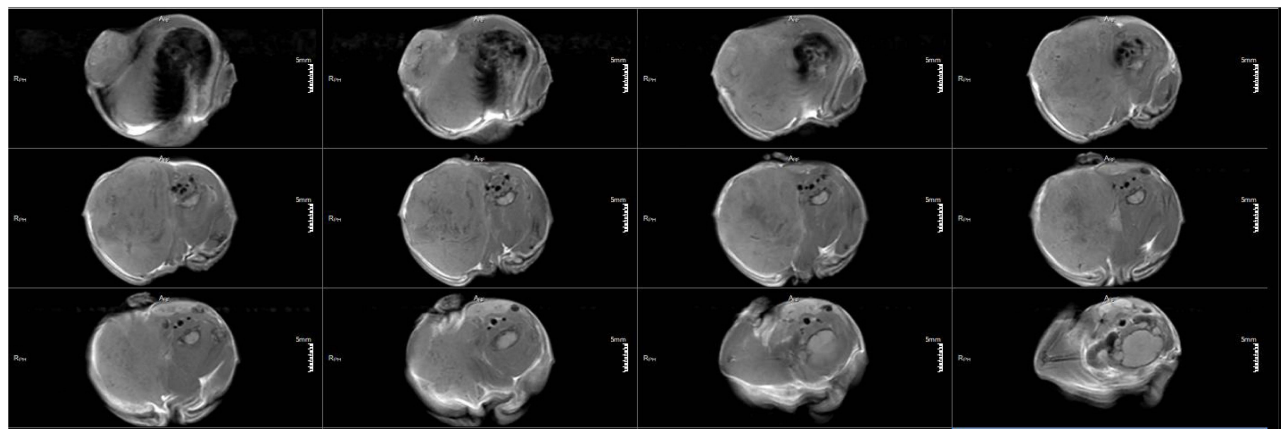
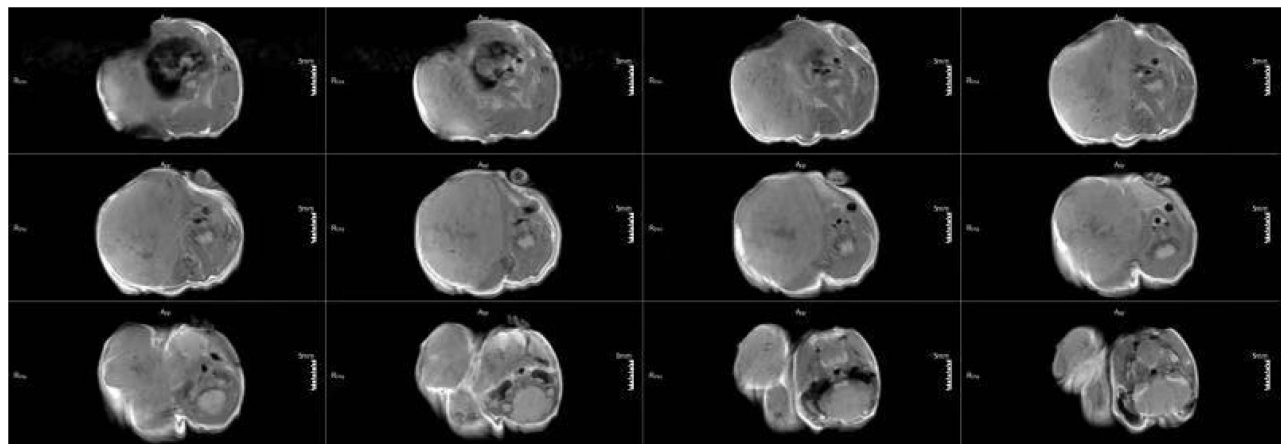


Figure 5 PPT experience scheme on the three cell lines treated with DOTA IN-CTL AuNPs (A). Temperature elevation in control (water, DOTA, and CTL solutions) and nanoparticles solution (DOTA IN-CTL AuNPs) during 15 min (B). Cell viability results (Mtt assay) in TIB-75, KKKU-M213 and Mia PaCa-2 cell lines treated with nanoparticles (right), before (grey) and after (red) irradiation at 808 nm wavelength laser at 0.75 W excitation power (C).

DOTA CTL AuNPs



DOTA



CTL

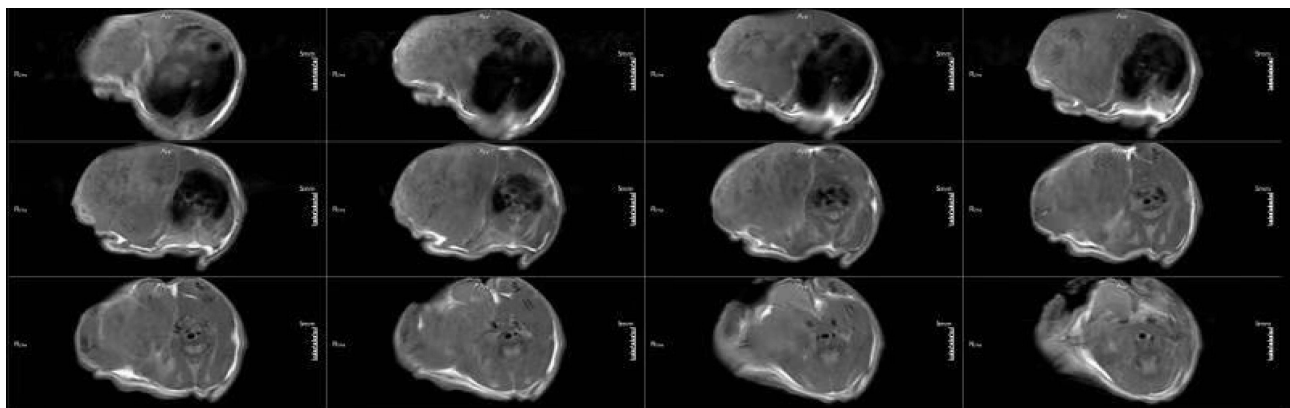


Figure 6 MRI images of T₁ weighting on tumor of DOTA-CTL-IN-AuNPs (at 1 h), DOTA (1 h) alone and CTL (1 h) alone recorded at 3T showing the efficient T₁ with hyper signal for DOTA IN-CTL AuNPs and DOTA alone.

and KKKU-M213 incubated with 2 nM DOTA IN-CTL AuNPs for 24 h before laser treatment. The cells were exposed to the same laser source (808 nm wavelength, 0.75 W/cm² power density) for 10 min. Figure 5C shows approximately 70% death in the case of irradiated cells in presence of nanoparticles (red bars) and 20% without nanoparticles (blue bars). As a control, the cells were incubated in phosphate buffered saline without nanoparticles (black bars) or incubated with nanoparticles, without laser exposition (grey bars). Note that in the case of TIB-75, the PTT is very efficient to kill 70% of the cells with or without nanoparticles.

MRI in vivo Preliminary Test

Figure 6 shows a clear bright contrast of the tumor on the images with DOTA alone and DOTA-CTL IN-AuNPs after 30 min of injection. We did not observe any enhancement of contrast after injection of CTL as a control.

To conclude, there is an efficient T₁ hyper signal with DOTA IN-CTL AuNPs and DOTA. So DOTA IN-CTL AuNPs can be an interesting new T₁ MRI contrast agent. Apart from this, we can assume that our nanovector will be a good candidate for further clinical applications after regular protocol testing.

Figure 7 and Table S1 show the biodistribution studies of DOTA and DOTA IN-CTL AuNPs on BALB/cA-Grade by MRI at 3T.

For this study we have monitored the ROI of a tumor and plotted the intensities of these regions. We can observe on the graph (in blue) that DOTA IN-CTL AuNPs arrives early (0.5 h) in the tumor compared to DOTA alone (1 h). The intensity of the signal for DOTA IN-CTL AuNPs is almost the same as DOTA alone. The clearance time for DOTA IN-CTL AuNPs is 1 h which is more rapid than DOTA alone (2 h). We can also see that there is total elimination of DOTA complexed nanoparticles after 2 h but for DOTREM the total elimination is greater than 2 h.

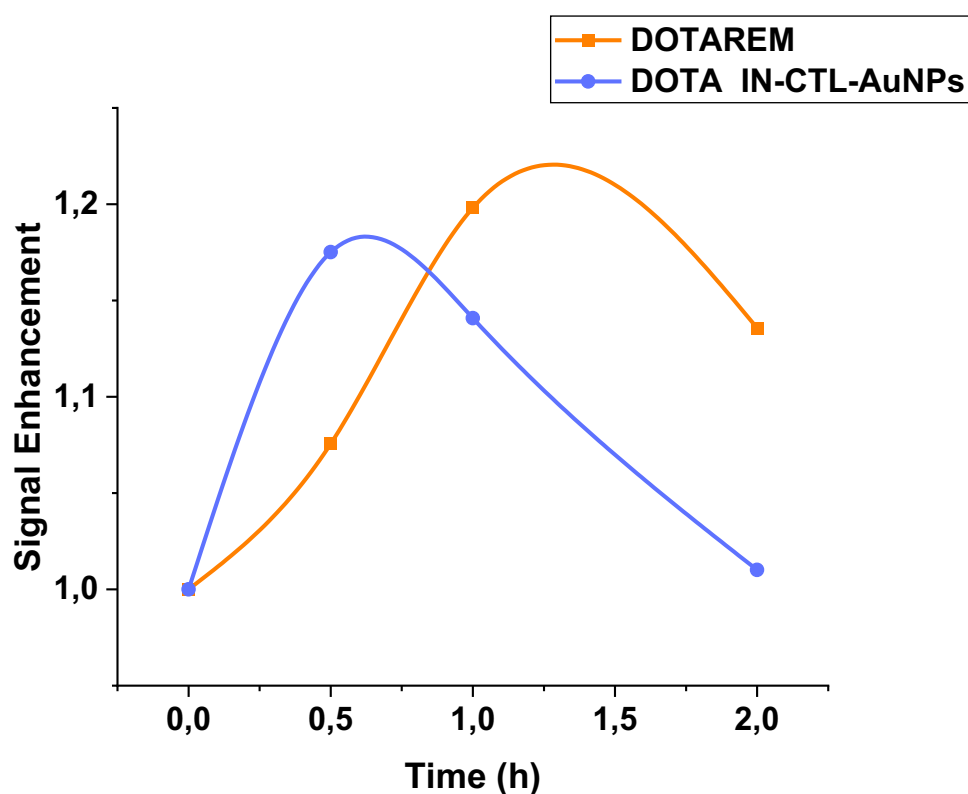


Figure 7 Biodistribution studies by dynamic contrast enhancement MRI on tumor.

Conclusion

In this paper, we developed, for the first time, novel hybrid nanoparticles as a contrast agent based of a Method IN strategy.⁹ In contrast to our previous works,^{10,15} DOTA was complexed with a gold salt, and then decorated by CTL polymer to improve biological activity and stability. Chemical-physical evaluations were carried out in order to elucidate the mechanism of hybrid nanostructure. We proved that DOTA IN-CTL AuNPs have several advantages: i) Biological efficacy on three cell lines: MIA PaCa-2 (human pancreatic cancer cell line), TIB-75 (murine liver cell line) and KKU-M213 (cholangiocarcinoma cell line); ii) high stability and no-toxicity; iii) high efficiency as a PPT agent. The study conducted on MRI in vitro and in vivo models will be suitable for diagnosis and therapy. Given these encouraging results, this DOTA hybrid-nanomaterial system constitutes a concrete promise as a therapeutic entity in the field of medicinal and clinical applications.

Acknowledgments

We thank “Ligue contre le Cancer” for financing MK’s thesis and making possible the development of this work. The MRI experiments were supported by Science and Technology Planning Project of Guangdong Province of China [no. 2020A1414010089], Natural Science Foundation of Guangdong Province of China [no. 2021A1515012161], Guangdong Province Regional Joint Fund-Key Projects [no. 2020B1515120096] and Sanming Project of Medicine in Shenzhen [no. SZSM202003009]. This work has been partly performed on the CNanoMat platform of the University Paris 13. We thank QiqianLiu (Univ-Paris13) for elaboration and discussion about in vivo preliminary study.

Disclosure

The authors report no conflicts of interest in this work.

References

1. Dreaden EC, Alkilany AM, Huang X, Murphy CJ, El-Sayed MA. The golden age: gold nanoparticles for biomedicine. *Chem Soc Rev*. 2012;41:2740–2779. doi:10.1039/c1cs15237h
2. Lou-Franco J, Das B, Elliott C, Cao C. Gold nanozymes: from concept to biomedical applications. *Nano-Micro Letters*. 2020;13:10. doi:10.1007/s40820-020-00532-z
3. Koya AN, Zhu X, Ohannesian N, et al. Nanoporous metals: from plasmonic properties to applications in enhanced spectroscopy and photocatalysis. *ACS Nano*. 2021;15:6038–6060. doi:10.1021/acsnano.0c10945
4. Jeong -H-H, Choi E, Ellis E, Lee T-C. Recent advances in gold nanoparticles for biomedical applications: from hybrid structures to multi-functionality. *J Mater Chem B*. 2019;7:3480–3496. doi:10.1039/C9TB00557A
5. Ai X, Mu J, Xing B. Recent advances of light-mediated theranostics. *Theranostics*. 2016;6:2439–2457. doi:10.7150/thno.16088
6. Zavaleta C, Ho D, Chung EJ. Theranostic nanoparticles for tracking and monitoring disease state. *SLAS Technol*. 2018;23:281–293. doi:10.1177/2472630317738699
7. Das P, Ganguly S, Margel S, Gedanken A. Tailor made magnetic nanolights: fabrication to cancer theranostics applications. *Nanoscale Adv*. 2021;3:6762–6796. doi:10.1039/D1NA00447F
8. Mortezaazadeh T, Gholibegloo E, Khoobi M, Alam NR, Haghighi S, Mesbahi A. In vitro and in vivo characteristics of doxorubicin-loaded cyclodextrine-based polyester modified gadolinium oxide nanoparticles: a versatile targeted theranostic system for tumour chemotherapy and molecular resonance imaging. *J Drug Target*. 2020;28:533–546. doi:10.1080/1061186X.2019.1703188
9. Moustaooui H, Movia D, Dupont N, et al. Tunable design of Gold(III)–Doxorubicin Complex–PEGylated nanocarrier. The golden doxorubicin for oncological applications. *ACS Appl Mater Interfaces*. 2016;8:19946–19957. doi:10.1021/acsami.6b07250
10. Khan M, Boumati S, Arib C, et al. Doxorubicin (DOX) gadolinium-gold-complex: a new way to tune hybrid nanorods as theranostic agent. *Int J Nanomed*. 2021;16:2219–2236. doi:10.2147/IJN.S295809
11. Liu Q, Liu H, Sacco P, et al. CTL–doxorubicin (DOX)–gold complex nanoparticles (DOX–AuGCs): from synthesis to enhancement of therapeutic effect on liver cancer model. *Nanoscale Adv*. 2020;2:5231–5241. doi:10.1039/D0NA00758G
12. Arib C, Spadavecchia J, de la Chapelle ML. Enzyme mediated synthesis of hybrid polyedric gold nanoparticles. *Sci Rep*. 2021;11:3208. doi:10.1038/s41598-021-81751-1
13. Arib C, Bouchemal N, Barile M, et al. Flavin-adenine-dinucleotide gold complex nanoparticles: chemical modeling design, physico-chemical assessment and perspectives in nanomedicine. *Nanoscale Adv*. 2021;3:6144–6156. doi:10.1039/D1NA00444A
14. Marguerit G, Moustaooui H, Haddada MB, Djaker N, de la Chapelle ML, Spadavecchia J. Taxanes hybrid nanovectors: from design to physico-chemical evaluation of docetaxel and paclitaxel Gold (III)–PEGylated complex nanocarriers. *Part Part Syst Charact*. 2018;35:1700299. doi:10.1002/ppsc.201700299
15. Aouidat F, Boumati S, Khan M, Tielens F, Doan B-T, Spadavecchia J. Design and synthesis of gold-gadolinium-core-shell nanoparticles as contrast agent: a smart way to future nanomaterials for nanomedicine applications. *Int J Nanomed*. 2019;14:9309–9324. doi:10.2147/IJN.S224805
16. Alric C, Taleb J, Le Duc G, et al. Gadolinium chelate coated gold nanoparticles as contrast agents for both X-ray computed tomography and magnetic resonance imaging. *J Am Chem Soc*. 2008;130:5908–5915. doi:10.1021/ja078176p

17. Moriggi L, Cannizzo C, Dumas E, Mayer CR, Ulianov A, Helm L. Gold nanoparticles functionalized with gadolinium chelates as high-relaxivity MRI contrast agents. *J Am Chem Soc.* **2009**;131:10828–10829. doi:10.1021/ja904094t
18. Irure A, Marradi M, Arnáiz B, Genicio N, Padro D, Penadés S. Sugar/gadolinium-loaded gold nanoparticles for labelling and imaging cells by magnetic resonance imaging. *Biomater Sci.* **2013**;1:658–668. doi:10.1039/c3bm60032g
19. Mortezaazadeh T, Gholibegloo E, Alam NR, et al. Gadolinium (III) oxide nanoparticles coated with folic acid-functionalized poly(β -cyclodextrin-co-pentetic acid) as a biocompatible targeted nano-contrast agent for cancer diagnostic: in vitro and in vivo studies. *Magma.* **2019**;32:487–500. doi:10.1007/s10334-019-00738-2
20. Hoshyar N, Gray S, Han H, Bao G. The effect of nanoparticle size on in vivo pharmacokinetics and cellular interaction. *Nanomedicine.* **2016**;11:673–692. doi:10.2217/nmm.16.5
21. Sacco P, Furlani F, Paoletti S, Donati I. pH-Assisted gelation of lactose-modified chitosan. *Biomacromolecules.* **2019**;20:3070–3075. doi:10.1021/acs.biomac.9b00636
22. Tweedle MF. The chemistry of contrast agents in medical magnetic resonance imaging. *J Am Chem Soc.* **2002**;124:884–885.
23. Wahsner J, Gale EM, Rodríguez-Rodríguez A, Caravan P. Chemistry of MRI contrast agents: current challenges and new frontiers. *Chem Rev.* **2019**;119:957–1057. doi:10.1021/acs.chemrev.8b00363
24. Clough TJ, Jiang L, Wong K-L, Long NJ. Ligand design strategies to increase stability of gadolinium-based magnetic resonance imaging contrast agents. *Nat Commun.* **2019**;10:1420. doi:10.1038/s41467-019-09342-3
25. Tirsós G, Kovacs Z, Sherry AD. Equilibrium and formation/dissociation kinetics of some Ln III PCTA complexes. *Inorg Chem.* **2006**;45(23):9269–9280. doi:10.1021/ic0608750
26. Baranyai Z, Tirsós G, Rösch F. The use of the macrocyclic chelator DOTA in radiochemical separations. *Eur J Inorg Chem.* **2020**;2020:36–56. doi:10.1002/ejic.201900706
27. Mueller R, Moreau M, Yasmin-Karim S, et al. Imaging and characterization of sustained gadolinium nanoparticle release from next generation radiotherapy biomaterial. *Nanomaterials.* **2020**;10(11):2249. doi:10.3390/nano10112249
28. Sacco P, Decleva E, Tentor F, et al. Butyrate-loaded chitosan/hyaluronan nanoparticles: a suitable tool for sustained inhibition of ROS release by activated neutrophils. *Macromol Biosci.* **2017**;17(11):4. doi:10.1002/mabi.201700214
29. Cok M, Sacco P, Porrelli D, et al. Mimicking mechanical response of natural tissues. Strain hardening induced by transient reticulation in lactose-modified chitosan (chitlac). *Int J Biol Macromol.* **2018**;106:656–660. doi:10.1016/j.ijbiomac.2017.08.059
30. Diallo AT, Tlemcani M, Khan M, Spadavecchia J, Djaker N. Size, shape, and wavelength effect on photothermal heat elevation of gold nanoparticles: absorption coefficient experimental measurement. *Part Part Syst Charact.* **2020**;37(12):2000255. doi:10.1002/ppsc.202000255
31. Moustauoui H, Saber J, Djeddi I, et al. Shape and size effect on photothermal heat elevation of gold nanoparticles: absorption coefficient experimental measurement of spherical and urchin-shaped gold nanoparticles. *J Phy Chem C.* **2019**;123:17548–17554. doi:10.1021/acs.jpcc.9b03122
32. Liu H, Jiang P, Li Z, Li X, Djaker N, Spadavecchia J. HIV-1 tat peptide-gemcitabine Gold (III)-PEGylated complex nanoflowers: a sleek thermosensitive hybrid nanocarrier as prospective anticancer. *Part Part Syst Charact.* **2018**;35:1800082. doi:10.1002/ppsc.201800082
33. Liu Y, Tang Y, Tian Y, et al. Gadolinium-doped hydroxyapatite nanorods as T1 contrast agents and drug carriers for breast cancer therapy. *ACS Appl Nano Mater.* **2019**;2:1194–1201. doi:10.1021/acsanm.8b02036
34. Cheheltani R, Ezzibdeh RM, Chhour P, et al. Tunable, biodegradable gold nanoparticles as contrast agents for computed tomography and photoacoustic imaging. *Biomaterials.* **2016**;102:87–97. doi:10.1016/j.biomaterials.2016.06.015
35. Liu Q, Sacco P, Marsich E, et al. Lactose-modified chitosan Gold(III)-PEGylated complex-bioconjugates: from synthesis to interaction with targeted Galectin-1 protein. *Bioconjug Chem.* **2018**;29:3352–3361. doi:10.1021/acs.bioconjchem.8b00520
36. Chen L, Chen JY, Qiu SS, et al. Biodegradable nanoagents with short biological half-life for SPECT/PAI/MRI multimodality imaging and PTT therapy of tumors. *Small.* **2018**;14.
37. Liu Y, Chang Z, Yuan HK, Fales AM, Vo-Dinh T. Quintuple-modality (SERS-MRI-CT-TPL-PTT) plasmonic nanoprobe for theranostics. *Nanoscale.* **2013**;5:12126–12131. doi:10.1039/c3nr03762b
38. Wu YZ, Xiong WF, Wang ZK, et al. Self-assembled MXene-based Schottky-junction upon transition metal oxide for regulated tumor microenvironment and enhanced CDT/PTT/MRI activated by NIR irradiation. *Chem Eng J.* **2022**;427. doi:10.1016/j.cej.2021.131925
39. Hatamie S, Balasi ZM, Ahadian MM, Mortezaazadeh T, Shams F, Hosseinzadeh S. Hyperthermia of breast cancer tumor using graphene oxide-cobalt ferrite magnetic nanoparticles in mice. *J Drug Deliv Sci Technol.* **2021**;65:102680. doi:10.1016/j.jddst.2021.102680
40. Abadeer NS, Murphy CJ. Recent progress in cancer thermal therapy using gold nanoparticles. *J Phy Chem C.* **2016**;120:4691–4716. doi:10.1021/acs.jpcc.5b11232
41. Cheng XJ, Sun R, Yin L, Chai ZF, Shi HB, Gao MY. Light-triggered assembly of gold nanoparticles for photothermal therapy and photoacoustic imaging of tumors in vivo. *Adv Mater.* **2017**;29:45.
42. Jaque D, Martínez Maestro L, Del Rosal B, et al. Nanoparticles for photothermal therapies. *Nanoscale.* **2014**;6:9494–9530. doi:10.1039/c4nr00708e